3*d* electron collapse in the $2p^5 3d$ configuration in argon-like ions

A. A. Maĭste, R. É. Ruus, and M. A. Élango

Institute of Physics, Estonian Academy of Sciences

(Submitted 28 March 1980)
Zh. Éksp. Teor. Fiz. **79**, 1671–1677 (November 1980)

The $L_{2,3}$ emission and absorption (or photoelectric quantum yield) spectra of K^+ in KF, KCl, KBr and KI, of Ca^{2+} in CaF_2 and $CaCl_2$, and of Sc^{3+} in Sc_2O_3 are measured (in part by using synchrotron radiation). It is shown that the onset regions of the absorption spectra are characterized by intense bands which have resonant partners in the corresponding emission spectra; these bands are associated with the $2p$–$3d$ transitions in the free ions K^+, Ca^{2+}, and Sc^{3+}. Comparison of the $L_{2,3}$ spectra of the isoelectronic sequence of argon-like ions (from Cl to Sc^{3+}) shows that 3*d* electron collapse in the $2p^5 3d$ configuration occurs in this sequence in the transitions $Ar \to K^+ \to Ca^{2+}$.

PACS numbers: 78.55.Fv, 72.40. + w

1. INTRODUCTION

The nonmonotonic change in the energy and spatial characteristics of electrons with large orbital angular-momentum quantum numbers ($l \geq 2$) as the atomic number of effective charge increases is one of the most interesting patterns associated with the build-up of atomic electron shells. The possibility of an abrupt contraction of the radial wave function, accompanied by a sharp increase in binding energy—the so-called electron (or orbital) collapse—is explained by the characteristics of the effective potential for such electrons.[1-4]

The collapse of an excited *nl* electron is apparent in two aspects in spectroscopic measurements. Firstly due to the increase in binding energy, the terms of the configuration with the collapsing electron sharply drop along the energy scale, crossing levels of other configurations. Secondly, due to contraction of the collapsing orbital, its overlap with subvalence orbitals located near the nucleus is increased; therefore the oscillator strengths of the corresponding transitions increase greatly.

The latter circumstance was used in the preceding work[4] to experimentally establish 4*f*-electron collapse. In this work we use it to study 3*d*-electron collapse (in the $2p^5 3d$ configuration in the isoelectronic sequence of argon-like ions), which according to theoretical estimates[3,5] has a number of peculiarities. We have proceeded from the premise established in recent years that the basic characteristics of the absorption spectra associated with transitions from subvalence shells of atoms or ions (especially positive ions) are preserved when they are introduced into compounds,[6-8] and we have investigated the $L_{2,3}(2p)$ absorption and emission spectra of K^+, Ca^{2+}, and Sc^{3+} in a number of compounds.

2. EXPERIMENTAL PART

The spectra were measured using an RSM-500 x-ray spectrometer-monochromator. Synchrotron radiation from the VEPP-2M storage ring. Institute of Nuclear Physics, Siberian Branch of the USSR Academy of Sciences, was used for measurement of the $\mu(h\nu)$ absorption spectra. In some cases instead of the $\mu(h\nu)$ spectra we measured the photoelectric quantum-yield (electron emission) spectra $\varkappa(h\nu)$, using the bremsstrahlung of the tungsten target cathode. The validity of such a substitution in study of the structure of the $\mu(h\nu)$ spectrum is well known and widely used when direct measurement of $\mu(h\nu)$ is impossible or inexpedient.[9] The $\varkappa(h\nu)$ spectra were measured relative to CsI, which does not have any appreciable structure in the region under study.[10] Instrument resolution for the $\mu(h\nu)$ and $\varkappa(h\nu)$ spectra was 0.3–0.6 eV.

In the case of the KCl absorption spectrum, it proved to be necessary to correct for scattered radiation; taking this into account (by measuring the transmission of KCl plates of different thicknesses with various detectors) we could refine the values of μ in the region of the principal maxima.

In the measurement of the emission spectra $I(h\nu)$, the samples were attached in the form of thin sheets to copper plates serving as the target cathode of the x-ray tube, and were covered with thin aluminum sheets which provided for some deceleration of the exciting electrons (in order to reduce reabsorption) and for protection from radiolysis in the more powerful operating regimes of the tube. The resolution was on the order of 1 eV.

On Fig. 1, we present $L_{2,3}$ absorption and emission spectra of K^+ in KCl, of Ca^{+2} in CaF_2, and of Sc^{3+} in Sc_2O_3 [in the latter case, the $\varkappa(h\nu)$ spectrum is given instead of the $\mu(h\nu)$ spectrum]. All the absorption spectra start with several intense and narrow (intrinsic half-width about 0.2–0.3 eV) maxima, followed by a less intense structure. In the low-energy regions of the emission spectra, there are broad maxima associated with transitions from the valence band of the corresponding crystals, and in the high-energy region there are bands which are resonant with the primary absorption bands.

On Fig. 2 we present the $\varkappa(h\nu)$ spectra of potassium halides in the $L_{2,3}$ absorption region of K^+. It is evident that in the case of KCl, the $\varkappa(h\nu)$ spectrum duplicates the shape of the $\mu(h\nu)$ spectrum in Fig. 1 quite well (taking into account the slightly lower resolution), and that the basic details of the onset region of the spectra are not very sensitive to the particular com-

0038-5646/80/110844-04$02.40

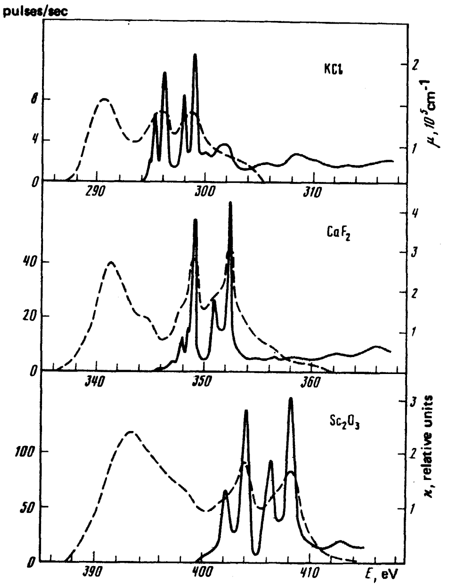

FIG. 1. $L_{2,3}$ emission spectra (dashed lines) and absorption spectra (solid lines) of potassium in KCl, calcium in CaF_2, and scandium in Sc_2O_3 (in the latter case, the $\varkappa(h\nu)$ spectrum is given instead of the $\mu(h\nu)$ spectrum—see text).

pound. Still greater similarity is observed for the absorption spectra of CaF_2 and $CaCl_2$.

The general features of our spectra agree with $\varkappa(h\nu)$ spectra of KCl and CaF_2 given in papers by other authors[11,12]; but due to the substantially higher resolution (achieved primarily as a result of the use of synchrotron radiation), our spectra contain significantly more detail. The $L_{2,3}$ emission spectrum of Ca^{2+} in CaF_2 given by Nemoshkalenko *et al.*[12] does not have bands which are resonant with the absorption bands—apparently due to an insufficient decrease of the self-absorption effects.

3. DISCUSSION OF RESULTS

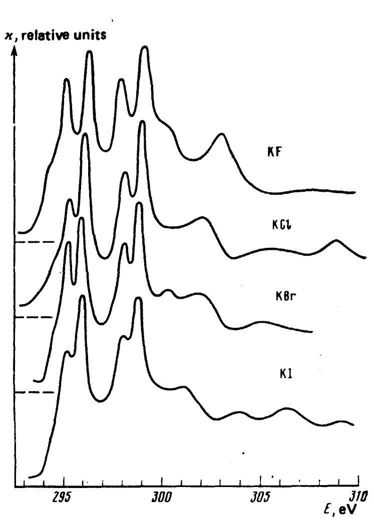

FIG. 2. Photoemission quantum yield $\varkappa(h\nu)$ spectra of potassium halides in the $L_{2,3}$-edge region of potassium.

TABLE I. Ionization energies of the $L_{2,3}$ shell, $2p-3d$, $4s$ transition energies in free argon-like ions and energies of the corresponding maxima in the $L_{2,3}$ absorption spectra of ionic crystals.

	$E(L_3)$	$E(L_2)$	$E(L_3-3d)$	$E(L_2-3d)$	$E(L_3-4s)$	$E(L_2-4s)$
Ar	248.6	250.7	246.9	249.0	244.2	246.3
Experiment (Ref. 16)	248.6	250.8	246.8	248.9	244.3	246.4
K^+	307.6	310.3	297.4	300.1	295.7	298.4
KCl			296.4	299.2		
Ca^{2+}	372.2	375.8	347.5	351.1	350.6	354.2
CaF_2			349.1	352.4		
Sc^{3+}	443.8	448.3	400.6	405.1	410.6	415.1
Sc_2O_3			403.8	408.0		

The high intensity of the structure in the onset region of the $\mu(h\nu)$ and $\varkappa(h\nu)$ spectra presented in Figs. 1 and 2, both in absolute units and relative to the structure in the higher energy region, does not leave any doubt that the intensity is due to dipole-allowed transitions—i.e., $2p-d$ and $2p-s$ transitions. In order to further interpret this structure, it is first of all necessary to establish if the wave function of the final state is primarily determined by the potential of the absorbing ion (in which the initial state is localized) or by the solid-state potential created by the environment.

It was shown above that experimental and theoretical information accumulated in recent years leads to the conclusion that both the ground and excited states of the cations in ionic crystals are determined primarily by the internal potential, and the so-called "solid-state effects" must be taken into account only in successive approximations.[6,8]

Our work confirms the correctness of this point of view. In Table I we give a comparison of the energies of the two most intense maxima of the $L_{2,3}$ absorption spectra of K^+ in KCl, Ca^{2+} in CaF_2, Sc^{3+} in Sc_2O_3 and Ar with the energies of the $2p-3d$ and $2p-4s$ transitions in the free K^+, Ca^{2+}, and Sc^{3+} ions and in the Ar atom, obtained according to the so-called "$Z+1$ scheme" (equivalent-cores approximation) as the difference between the ionization energy of the $L_{2,3}$ shell of the free ion (or atom) with the given Z $[E(L_{2,3})]$ and the binding energies of the $3d$ and $4s$ levels of the $Z+1$ ion $[E(3d, 4s)]$. We may estimate $E(L_{2,3})$, using data on energies of atomic levels[13] and ionization potentials (Ref. 14, p. 20); $E(3d, 4s)$ are tabulated.[15] For Ar we also present results of direct experimental determination[16] of $E(L_{2,3})$, $E(2p-3d)$, and $E(2p-4s)$. It is evident from Table I that the energy estimates found for transitions in free ions (accurate to within 1-3 eV) coincide with the energies of the most intense maxima of the corresponding solid-state absorption spectra. Consequently, the energetics of the transitions under consideration in ionic crystals are determined primarily by the energetics of the corresponding transitions in free ions. We also note that the principal maxima of the K^+ and Ca^{2+} absorption spectra presented here agree within 0.5 eV with the principal maxima of the $L_{2,3}$ absorption spectra of potassium and calcium vapors, as measured in Ref. 17.

If the final d and s states of the transitions under consideration were to be transformed into conduction-band states of the corresponding crystals, it would be extremely difficult to explain the similarity of the KCl spectrum to the KF, KBr, and KI spectra (Fig. 2) and

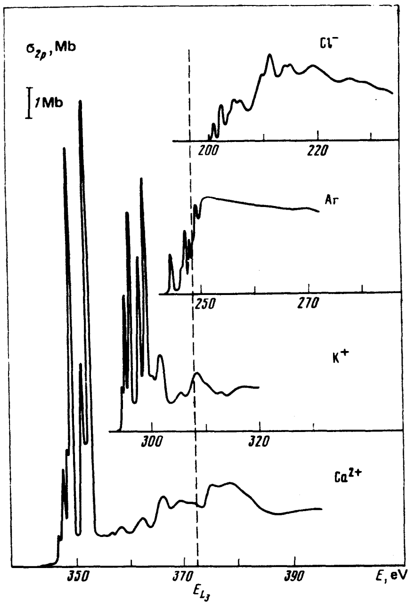

FIG. 3. Photoabsorption cross sections of the argon-like ions Cl$^-$, Ar, K$^+$, and Ca^{2+} in the $L_{2,3}$-edge region.

its sharp difference from the $L_{2,3}$ spectrum[18] of Cl$^-$ in KCl (Fig. 3) and the $M_{2,3}$ spectrum[19] of K$^+$ in KCl.

Thus, the onset structure of $L_{2,3}$ absorption spectra of K$^+$, Ca^{2+}, and Sc^{3+} in ionic crystals is determined primarily by the $2p-3d$ and $2p-4s$ transitions in the corresponding free ions. From Table I it follows that a fundamental role is played there by the $2p-3d$ transitions. The $2p-4s$ transitions may play some role in the K$^+$ case; their intensity is low, however, indicated by the Ca^{2+} and Sc^{3+} spectra (in which the energies of the $2p^53d$ and $2p^54s$ configurations differ appreciably). Furthermore, in the hydrogen model of the atom, the oscillator strength of the $p-d$ transitions exceeds the oscillator strength of the $p-s$ transitions by an order of magnitude.[20]

A more detailed interpretation of the spectra presented is not essential from the point of view of this work. In order to carry out such an interpretation, detailed calculations are necessary, with account taken of several types of interactions having similar orders of magnitude (spin-orbit splitting of the $2p$ shell), splitting of $3d$ levels in the crystal field, electron-hole interaction, mixing of $2p^53d$ and $2p^54s$ configurations).

Let us proceed onward to a discussion of spatial localization of $3d$ orbitals in the $2p^53d$ configuration in the ions under consideration. First of all, we note that for Sc, even in the ground state, the orbital is localized within the inner electron shell region (Ref. 14, p. 28)—i.e., it is collapsed. The high intensity of the $2p$-$3d$ transitions and the presence of resonant bands on the $\varkappa(h\nu)$ and $I(h\nu)$ spectra observed in our work correspond to this. An analogous situation in the $\mu(h\nu)$ and $I(h\nu)$ spectra of K$^+$ and Ca^{2+} ions is evidence that $3d$-orbital collapse has already occurred in these ions.

In order to study the dynamics of $3d$-electron collapse in the isoelectonic sequence of argon-like ions, we present together in Fig. 3 the $L_{2,3}$ absorption spectra of Cl$^-$ (in KCl–Ref. 18), Ar(Ref. 16), K$^+$, and Ca^{2+}, given as plots of the photoabsorption cross section σ vs. photon energy. The dashed line indicates the ionization energy $E(L_3)$ of the L_3 subshell of the corresponding free ions (see Table I). Of course, $E(L_3)$ is not the energy separation between the L_3 subshell and the bottom of the conduction band in the crystal. It is given to demonstrate the change in binding energy of $3d$ states in the ions. The fact that the first maxima of the $L_{2,3}$ spectrum of Cl$^-$ in KCl, having an exciton character, are located above $E(L_3)$ shows that the free-ion approximation is not applicable to the interpretation of spectra of anions in ionic crystals. Nevertheless, the envelope of the $L_{2,3}$ absorption spectrum is similar for all chlorides[21] and reflects to some degree the properties of the $\sigma(h\nu)$ function for the free Cl$^-$ ion.

From Fig. 3 it is evident that the spectra for Cl$^-$ and Ar are radically different from the spectra for K$^+$ and Ca^{2+}. These measurements are interpreted well from the point of view of $3d$-orbital collapse in the ions of the sequence under consideration. Since these orbitals are located far from the nucleus (in the case of Cl$^-$ and Ar), the maximum of the photoabsorption cross section is attained in the continuum region of the spectrum. As Z increases, the oscillator strength is shifted closer to the absorption threshold and increases in absolute magnitude. On going to K$^+$, the role of the $2p-3d$ transitions sharply increases; they completely dominate in the spectrum. In the case of Ca^{2+}, the pattern is primarily the same, but the intensity of the principal maxima increases even more. The intensity of the resonant emission bands increases in the same direction (Fig. 1). All of the data presented show that the sharp contraction of the $3d$ orbitals begins on going from Ar to K$^+$ and is continued on going from K$^+$ to Ca^{2+}.

Thus, the data presented show that, in the isoelectronic sequence of argon like ions, $3d$-orbital collapse in the $2p^53d$ configuration occurs in the Ar → K$^+$ → Ca^{2+} sequence. It occurs somewhat more slowly than the $4f$-orbital collapse in the sequence of xenon-like ions, as was predicted by theory.[3,5]

Application of the above discussion to experimental data of Barinskii and Kulikova[22] leads to the conclusion that $4d$-orbital collapse in the $2p^54d$ configuration occurs in the isoelectronic Kr → Rb$^+$ → Sr^{2+} sequence of krypton-like ions.

According to the solid-state classification of electronic excitations, the intense maxima at the threshold of all the spectra under consideration correspond to the so-called x-ray excitons. The energy separation between the L_3 subshell of the cation and the bottom of the conduction band, estimated on the basis of data from x-ray photoelectron and optical spectroscopy, is about 299 eV and 352 eV respectively in potassium and calcium halides. The fact that such excitonic states differ little from the corresponding free-ion states is well understood on the basis of the picture presented above for $3d$-orbital collapse. The radius of such an orbital (according to the maximum of the charge density distribution) for $Z \approx 20$ is about 0.6 Å—i.e., about equal to the radius of the inner $3p$ shell of the ion in the ground state (Ref. 14, p. 31). The $2p-3d$ transition occurs practically within the cation (the ionic radii of K^+, Ca^{2+}, and Sc^{3+} are respectively 1.3, 1.0, and 0.8 Å). Therefore for such transitions, the situation on the crystal is not much different from the situation in the free ion, and the effect of the environment may be considered as a perturbation (for example, within the framework of ligand field theory). This was confirmed for the $3p$ spectra of K^+ and the $4p$ spectra of Rb^+ in alkali halide compiunds.[23,24] The situation is different in the case of $s-p$ and $p-s$ transitions; in K^+, for example the $1s-4p$ transition leads to almost a three-fold increase in the ionic radius, and the radius of the excited free ion already exceeds the radius of the cation sphere in the crystal. Solid-state effects are already significant in the corresponding spectra.

The authors thank E. S. Gluskin and A. P. Zhurakovskiĭ for help with the synchrotron radiation experiments, and A.M.-E. Saar for useful discussions.

[1] E. Fermi Scientific Works, Part 1 (Russ. Transl, Nauka, 1971, p. 298).
[2] M. Goeppert-Mayer, Phys. Rev. **60**, 184 (1941).
[3] D. C. Griffin, K. L. Andrew, and R. D. Cowan, Phys. Rev. **177**, 62 (1969).
[4] A. A. Maiste, R. É. Russ, S. A. Kuchas, R. I. Karaziya, and M. A. Élango, Zh. Eksp. Teor. Fiz. **78**, 941 (1980). [Sov. Phys. JETP **51**, 474 (1980)].
[5] S. A. Kuchas and A. B. Karosene, Lit. Fiz. Sbornik **18**, 187 (1978).
[6] V. I. Nefedov, Zh. Strukt. Khim. **11**, 299 (1970).
[7] T. M. Zimkina and A. S. Vinoradov, J. Phys. (Paris), Colloq. **32**, Suppl. 10, C4-278 (1971).
[8] B. Sonntage, J. Phys. (Paris) **39**, Suppl. 7, C4-9 (1978).
[9] T. M. Zimkina and V. A. Fomichev, Ul'tramyagkaya rentgenovskaya spektroskopiya (Ultrasoft X-Ray Spectroscopy), Izadt. Leningrad. Univ., Lenigrad, 1971, p. 33.
[10] A. P. Lukirskiĭ, E. P. Savinov, I. A. Brytov, and Yu. F. Shepelev, Izv. Akad. Nauk SSSR, Ser. Fiz. **28**, 866 (1964).
[11] A. P. Lukirskiĭ and T. M. Zimkina, Izv. Akad. Nauk SSSR, Ser. Fiz. 28, 765 (1964).
[12] V. V. Nemoshkalenko, Yu. N. Romashchenko, V. G. Aleshin, I. A. Brytov, and K. K. Sidorin, Izv. Akad. Nauk SSSR, Ser. Fiz. **38**, 626 (1974).
[13] J. A. Bearden and A. F. Burr, Rev. Mod. Phys. **39**, 125 (1967).
[14] G. V. Samsonov, ed., Svoĭstva élementor. Speravochnik. Chast' I. (Properties of the Elements. Handbook. Part I), Metallurgiya, 1976.
[15] C. E. Moore, Atomic Energy Levels, Vol. 1, U. S. National Bureau of Standards, Circular No. 467, U. S. Government Printing Office, Washington, D. C., 1949-1958.
[16] R. Haensel, G. Keitel, N. Kosuch, U. Nielsen, and P. Schreiber, J. Phys. (Paris), Colloq. **32**, C4-236 (1971).
[17] M. W. Mansfield, Proc. Roy. Soc. Lond. **A346**, 555 (1975); *ibid* **A348**, 143 (1976).
[18] F. C. Brown, C. Gähwiller, H. Fujita, A. B. Kunz, W. Scheifley, and N. Carrera, Phys. Rev. **B2**, 2126 (1970).
[19] U. Fano and J. W. Cooper, Spectral Distribution of Atomic Osicllator Strengths, Rev. Mod. Phys. **40**, 441-507 (1968) (Russ. Transl., Nauka, 1972, p. 66).
[20] H. Saito, M. Watanabe, A. Ejiri, S. Sato, H. Yamashita, T. Shibaguchi, H. Nishida, and S. Yamaguchi, Solid State Commun. **8**, 1861 (1970).
[21] A. M.-E. Saar and M. A. Élango, Fiz. Tverd. Tel. (Lenigrad) **13**, 3532 (1971). [Sov. Phys. Solid State **13**, 2985 (1971)].
[22] R. L. Barinskiĭ and I. M. Kulikova, Izv. Akad. Nauk SSSR, Ser. Fiz. **40**, 279 (1976).
[23] C. Satoko, Solid State Comm. **13**, 1851 (1973).
[24] C. Satoko and S. Sugano, J. Phys. Soc. Japan **34**, 701 (1973).

Translated by Cathy Flick

Laser interferometer with wavefront-reversing mirrors

N. G. Basov, I. G. Zubarev, A. B. Mironov, S. I. Mikhaĭlov, and A. Yu. Okulov

P. N. Lebedev Physics Institute, Academy of Sciences of the USSR, Moscow

(Submitted 1 April 1980)
Zh. Eksp. Teor. Fiz. **79**, 1678–1686 (November 1980)

A theoretical and experimental investigation was made of a Michelson interferometer with wavefront-reversing mirrors based on stimulated Brillouin scattering. It is shown that the period of the interference pattern obtained when the length of one of the interferometer arms is varied represents the frequency shift due to the stimulated scattering; the visibility curve tends to approach the limit 0.25 and represents a combination of the correlation functions for radiations with different path lengths corresponding to single and double transits across the difference between the interferometer arms. The interferometer can be used for any spatial structure of the exciting radiation and it is insensitive to the optical quality of its components.

PACS numbers: 07.60.Ly, 42.78.Dg, 42.60.By

1. INTRODUCTION

Reversal of laser radiation wavefront by nonlinear optics methods is attracting considerable attention. This is primarily due to the unique properties of the radiation reflected from wavefront-reversing mirrors, whose field is identical (apart from the phase factor) with the complex conjugate of the incident-wave field:

$$E_{\rm refl}(r_\perp)=\text{const}\,E^{*}_{\rm inc}(r_\perp).$$

The operation of complex conjugacy is equivalent to reversal of the direction of time in the Maxwell equations and the reflected wave traveling in the opposite direction passes consecutively through all the states